# Matched Reassignment of the Ultrasound Data of Breast Lesions

MASK11 Bachelor's Degree Project in Mathematical Statistics

Author
**Robert Vujasic**
ro6416vu-s@student.lu.se

Thesis Advisor
**Maria Sandsten**
maria.sandsten@matstat.lu.se

September 7, 2022

# Abstract

The goal of this thesis was to, from several randomly selected patients with diagnosed malignant and benign tumors, record optimal lambdas and respective Renyi entropies for each lambda, run a basic statistical analysis of the results and see if there is any significant difference between lambdas/Renyi entropies of malignant and benign lesions.

The results showed no significant difference.

The reassignment technique is a method that moves the signal energy to the center of gravity, giving higher energy concentration at the instantaneous frequency of the signal. The novel matched reassigned spectrogram method (MRS) was recently invented, with the goal to localize and classify transient functions of arbitrary shape. It was tailored for very short oscillating transients, which, theoretically, gives perfect reassignment localization to one single point in the time-frequency (TF) plane. Renyi entropy was used as concentration measure, where $\lambda$ is its minimizing parameter.

MATLAB algorithm for matched reassigned spectrogram was run on the OASBUD dataset that contains the raw radio-frequency echoes of breast lesions, recorded in two scan planes, along with their respective regions of interest (ROI), and classification of malignancy of the lesion for each patient.

# Contents

# 1 Introduction

Breast cancer is the most common cancer in women [7], and ultrasound plays and important role in its diagnosis, especially in differentiating between malignant and benign tumors. Nowadays, quantitative ultrasound (QUS) is becoming an important tool in breast lesion classification. It enables the estimation of tissue specific properties contained in the received echoes from the tissue under examination. However, the raw radio-frequency (RF) ultrasonic echoes are difficult to obtain in clinical practice, since the acquisition demands a dedicated ultrasound scanner. The Open Access Series of Breast Ultrasonic Data (OASBUD), is a set of radio-frequency signals which were recorded from breast lesions and are available for studying the specificity of the ultrasonic backscattered echoes from malignant and benign breast lesions. For each lesion, two individual longitudinal and transverse scan planes, radial scanning around the nipple, and antiradial scan planes were done. Two perpendicular scans (longitudinal and transverse) were recorded for every breast lesion, using the ultrasound scanner with centre frequency of 10 MHz.

Each scan consists 510 RF echo lines. The number of samples in every RF signal depended on the chosen penetration depth, and signals were digitized with 40 MHz sampling frequency. For each scan, the ROI logical matrix has exactly the same size as the matrix which contains the RF signals. The array multiplication of the RF file and the ROI file (value one within the ROI and zero outside) removes from the resulting array any data corresponding to the surrounding tissues and leaves only the echoes related to the pathological region

The specific region of interest (ROI) was specified by the radiologist for each lesion scan.

In this thesis we will attempt to examine the RF signals using the matched reassigned spectrogram method, which gives reassignment localization to one single point in the time-frequency (TF) plane. We will use Renyi entropy (defined in the next section) as the concentration measure, with $\lambda$ being its minimizing parameter. Four patients were randomly selected, two diagnosed with malignant tumor, and two with benign. The following process was applied for each separate patient: ROI and RF matrices were multiplied to leave us with only relevant echoes related to the pathological region. For each echo line, the optimal lambda was com-

puted and saved in a vector. Same was done for the corresponding Renyi entropies. Then we ran a basic statistical analysis (standard measures of location and spread). Same process was repeated on reduced datasets, where only 15 consecutive echo lines were selected for each patient, with the addition of computed correlation coefficients. This was done for both scan planes, RF1 and RF2, and the results were compared in an attempt to see whether or not there exist differences between malignantly and benignly classified lesions.

The ultrasonic RF echoes contained in the OASBUD file were recorded in the Department of Ultrasound, Institute of Fundamental Technological Research, Polish Academy of Science.

## 2 Matched Reassigned Spectrogram

The reassignment method is a technique that moves the signal energy to the center of gravity, giving higher energy concentration at the instantaneous frequency of the signal. The matched reassigned spectrogram (MRS),theoretically gives perfect instantaneous time and frequency localization, i.e. reassignment localization to one single point in the TF plane.
The short-time Fourier transform (STFT) of the oscillating transient signal

$$x(t) = a(t - t_0)e^{-\omega_0 t + \Phi}$$

using the window $h(t)$ is

$$F_x^h = \int_{-\infty}^{\infty} x(s)h^*(s - t)e^{-i\omega s}ds$$

where $^*$ is the complex conjugate and $\Phi$ is a phase. The corresponding spectrogram is found

$$S_x^h(t, \omega) = |F_x^h(t, \omega)|^2.$$

The reassigned spectrogram, where the spectrogram values are relocated to the corresponding $\hat{t}_x$ and $\hat{\omega}_x$, is defined as

$$RS_x^h(t, \omega) = \iint \; S_x^h(s, \xi)\delta(t - \hat{t}_x(s, \xi), \omega - \hat{\omega}_x(s, \xi))ds\frac{d\xi}{2\pi}$$

with $\iint \; f(t, \omega)\delta(t - t_0, \omega - \omega_0 dt d\omega/2\pi) = f(t_0, \omega_0)$, all integrals being from $-\infty$ to $\infty$. As the quadratic class of distributions obey TF shift-invariance, all analysis can be restricted to $x(t) = a(t)$, with time- and frequency center $t_0 = \omega_0 = 0$. The reassignment vectors for the matched window case, $h(t) = a(-t)$, are computed as

$$\hat{t}_x(t, \omega) = t + c_t\Re\left(\frac{F_x^{th}(t, \omega)}{F_x^h(t, \omega)}\right) = t - c_t\frac{t}{2}$$

$$\hat{\omega}_x(t, \omega) = \omega + c_\omega\Im\left(\frac{F_x^{\frac{dh}{dt}}(t, \omega)}{F_x^h(t, \omega)}\right) = \omega - c_\omega\frac{\omega}{2}$$

where $\Re(\cdot)$ and $\Im(\cdot)$ represent the real and imaginary parts, and $F_x^h(t, \omega)$, $F_x^{\frac{dh}{dt}}(t, \omega)$ are STFTs of the signal $x(t)$, with $t \cdot h(t)$ and $dh(t)/dt$ as window functions. The scaled reassignment, $c_t = c_\omega = 2$, reassigns all signal energy to $\hat{t}_x(t, \omega) = 0$, $(t_0)$ and $\hat{\omega}_x(t, \omega) = 0$, $(\omega_0)$.

Renyi entropy measure, used as the concentration measure of the MRS, of order $\alpha$ is defined as

$$RS_x^h(\lambda) = \frac{1}{1-\alpha} log_2 \int_{t_0}^{t_1} \int_{\omega_0}^{\omega_1} (RS_x^{h(\lambda)}(t,\omega))^\alpha dt d\omega,$$

using $\alpha = 3$.

# 3 Ultrasound Data and Analysis

We will explain the process of algorithm implementation and obtaining the results. The whole process is repeated for both of the scan planes, RF1 and RF2. For every patient selected, the RF matrix was multiplied by the ROI logical matrix to clean the data and leave us only with the data relevant for analysis. The region of interest was then "combed" to find the beginning and the end of the region of interest for each line. That was saved in the Ysig matrix. Fast Fourier transform length was set at 1024, and the sampling frequency at 40 MHz, according to [2]. Frequency range is chosen to be 3 MHz to 7 MHz. According to [2] it should be 10 MHz, but it doesn't match the observations, and 3 to 7 MHz is the region where things "seem to happen", so that was the reason for choosing it. Then the time and frequency bins were computed, and they decide the time and frequency limits for finding a peak. Time bins were selected to be the whole region of interest, just so we're able to capture the strongest possible peak and not risk the strongest peak being outside of the region. That region, illustratively shown for Patient 1, RF1, line 300 is shown in Figure 1, as the red box.

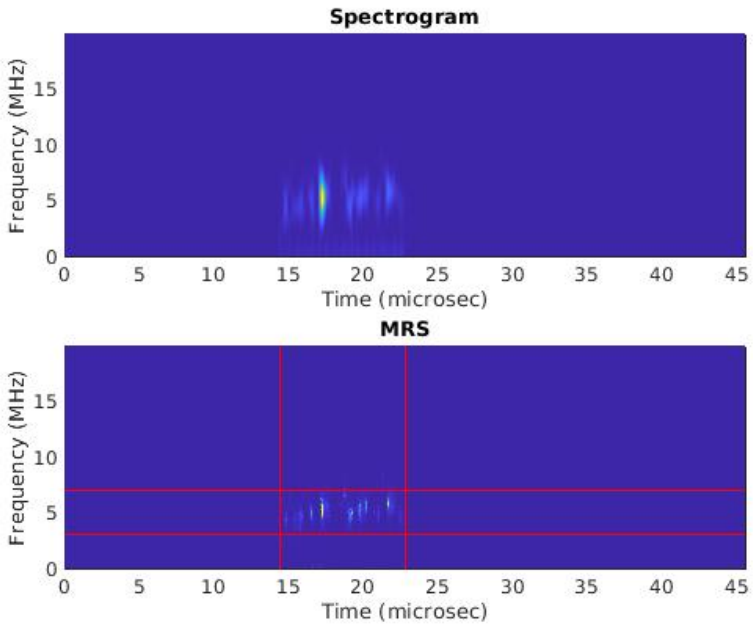


Figure 1: MRS with time and frequency bins (Patient 1, RF1 echo, line 300)

That is the region where the Renyi entropy is calculated for each lambda.

Next, we computed the matched reassigned spectrogram (MRS) with parameters described above. Although the MRS is very sensitive to the choice of lambda, in the interest of getting the best possible estimate of the optimal lambda for each line, lambdas in the range of 1 to 30 have been tested. For each optimal lambda the Renyi entropy is computed. Both lambdas and the corresponding Renyi entropies are then saved in their respective vectors on which the classification was performed later.

And finally, the spectrogram and matched reassigned spectrogram images are produced (single line example shown in Figure 1). The same process was repeated for all four selected patients.

Patients were selected randomly, two with diagnosed malignant tumors (Patient 4 and Patient 69), and two with diagnosed benign tumors (Patient 1 and Patient 23). Only four patients were selected to shorten the computation time. The idea was to see if there is an observable difference in distributions, means, variances and standard deviations of optimal lambdas and their corresponding Renyi entropies, for both scan planes RF1 and RF2, between malignant

and benign lesions.

The analysis was done on two different datasets. The full dataset, containing the optimal lambdas and corresponding Renyi entropies for every RF echo line in the region of interest, and the shortened dataset, where, observing the mesh grids of the data, 15 lines per scan plane per patient were selected in such a way that they capture the strongest peak of the grid.

Important thing to mention is that when optimal lambda equals 1, it is treated as an outlier. Due to inability to effectively deal with those outliers equally in both full and shortened datasets, because of the reasoning for taking specific lines in shortened datasets, they have been left in. There is a possibility that they skew the results, but we don't know by how much.

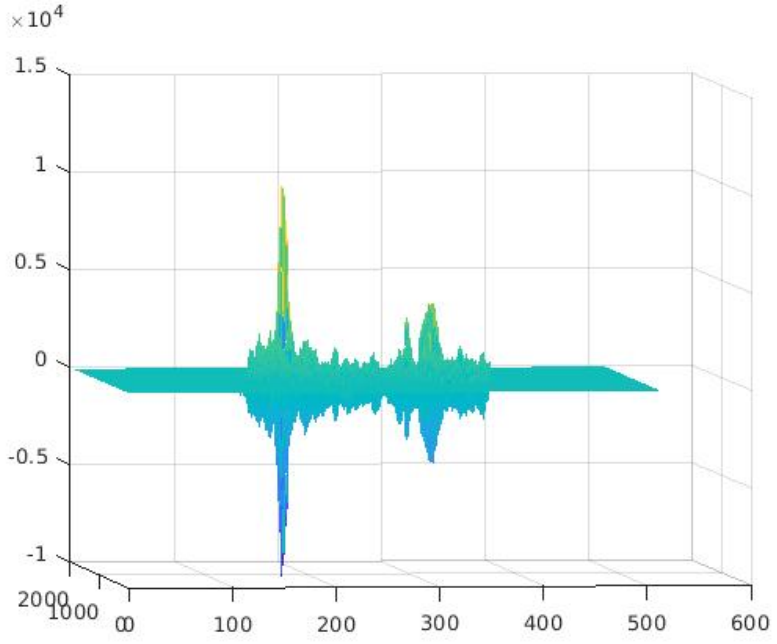


Figure 2: Mesh grid for cleaned up data of patient 1

### 3.1 KS density, mean, variance and standard deviation

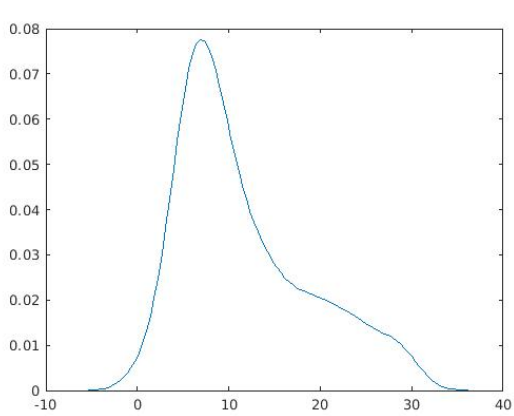


(a) KS density of lambdas, patient 1, RF1

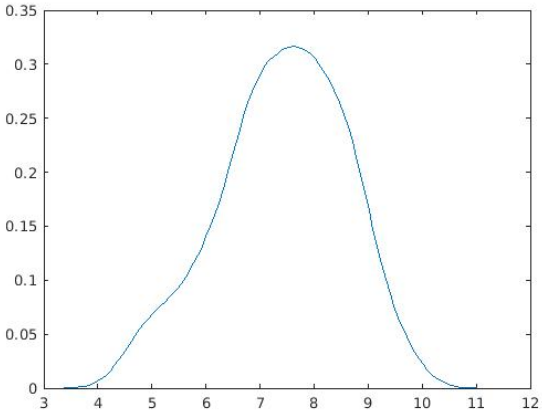


(b) KS density of Renyi entropies, patient 1, RF1

Figure 3: KS densities of lambdas and Renyi entropies for patient 1 (benign)

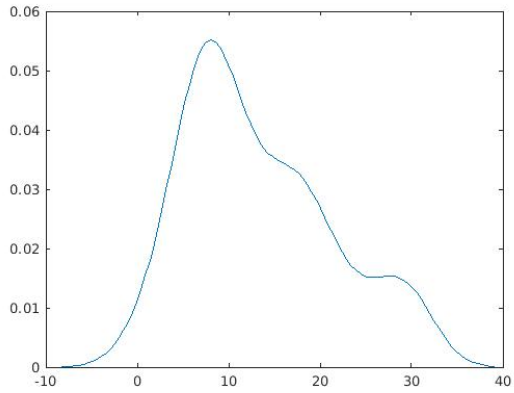


(a) KS density of lambdas, patient 4, RF1

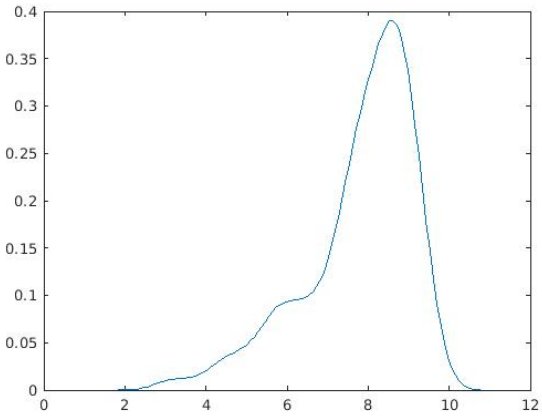


(b) KS density of Renyi entropies, patient 4, RF1

Figure 4: KS densities of lambdas and Renyi entropies for patient 4 (malignant)

Kernel smoothing (KS) function estimate for univariate and bivariate data is used to produce probability density estimates of optimal lambdas and corresponding Renyi entropies.

The following is the description of the function from [8]. MATLAB function

**[f,xi] = ksdensity(x)** returns a probability density estimate, f, for the sample data in the vector or two-column matrix x. The estimate is based on a normal kernel function, and is evaluated at equally-spaced points, xi, that cover the range of the data in x. ksdensity estimates the density at 100 points for univariate data, or 900 points for bivariate data.

To preface the analysis, ksdensity produced graphs where, in some cases, the density function crossed into negative values, which cannot be the case. Since we couldn't find a better MATLAB function to estimate densities of optimal lambda and Renyi entropy vectors, we stuck with using ksdensity.

We will first observe the results of the analysis on the full dataset.

As seen in the Figure 3 and Figure 4, KS distributions of optimal lambdas look fairly similar, for both the patient with a malignant tumor and the one with benign tumor. They have roughly the same mean and shape, with variance of optimal lambdas of patient 4 being observably larger than that of patient 1.

KS densities of corresponding Renyi entropies, however, look noticeably different, despite having a very similar mean, with that of patient 1 being more centered and broad, and of patient 4 being narrow and slightly left-skewed.

Table 1: Mean, variance and standard deviation for optimal lambda for the full dataset

| **PATIENT** | **mean** | **var** | **std** | **Classification** |
|---|---|---|---|---|
| Patient 1 RF1 | 11.6349 | 50.1328 | 7.0805 | Benign |
| Patient 1 RF2 | 13.0155 | 46.3055 | 6.8048 | Benign |
| Patient 4 RF1 | 13.3427 | 62.1813 | 7.8855 | Malignant |
| Patient 4 RF2 | 12.4068 | 58.0722 | 7.6205 | Malignant |
| Patient 23 RF1 | 12.2362 | 56.1342 | 7.4923 | Benign |
| Patient 23 RF2 | 11.3462 | 58.2123 | 7.6297 | Benign |
| Patient 69 RF1 | 11.9259 | 51.7328 | 7.1926 | Malignant |
| Patient 69 RF2 | 11.9259 | 50.9808 | 7.1401 | Malignant |

The observation is corroborated by the data in Table 1 and Table 2. When we observe the means of optimal lambdas, the means for patient 4 (malignant) are slightly higher than for patients 1 and 23 (both benign), but for patient 69 (malignant) means are the lowest of the whole group, so it implies that the mean of optimal lambda can't be a useful metric, given the discrepancy. Same conclusion can be drawn for standard deviations as well, since they follow the same pattern. The only significant difference can be observed in variance, where the variance of optimal lambdas for patients with benign tumors is significantly lower than for those with malignant tumors, so studying variance of optimal lambdas could be a step in the right direction.

As for Renyi entropies, the difference in KS densities between the patient 1 and patient 4 is easily observable in Figures 2 and 3, and could point out to narrower and more skewed KS densities indicating malignancy of the lesion, but the data for patient 69 throws this conclusion off, because KS densities in both RF1 and RF2 echo planes are pretty even and centered, without prominent tails on any end. For that reason, we won't conclude that the distribution of Renyi entropies gives us a good indication of lesion's malignancy.

Table 2: Mean, variance and standard deviation for optimal Renyi entropy for the full dataset

| **PATIENT** | **mean** | **var** | **std** | **Classification** |
|---|---|---|---|---|
| Patient 1 RF1 | 7.4115 | 1.3297 | 1.1513 | Benign |
| Patient 1 RF2 | 7.8007 | 1.0545 | 1.0269 | Benign |
| Patient 4 RF1 | 7.7879 | 1.7740 | 1.3319 | Malignant |
| Patient 4 RF2 | 7.5829 | 1.0518 | 1.0256 | Malignant |
| Patient 23 RF1 | 7.5813 | 7.4923 | 1.0036 | Benign |
| Patient 23 RF2 | 7.2200 | 1.1186 | 1.0576 | Benign |
| Patient 69 RF1 | 7.5325 | 0.6041 | 0.7772 | Malignant |
| Patient 69 RF2 | 7.5325 | 0.9917 | 0.9959 | Malignant |

We will also present KS densities of optimal lambdas/Renyi entropies plotted together.

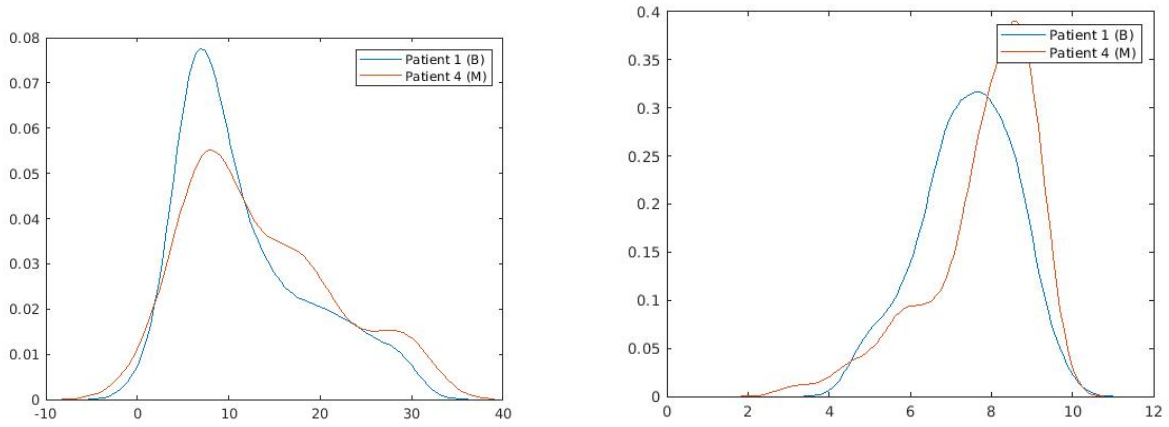


(a) KS density of optimal lambdas, RF1

(b) KS density of Renyi entropies, RF1

Figure 5: KS densities of lambdas and Renyi entropies for full dataset of patients 1 and 4

Now we will look at shortened datasets, where lines were selected in such a way to capture

the strongest peak of the mesh grid of the original data.

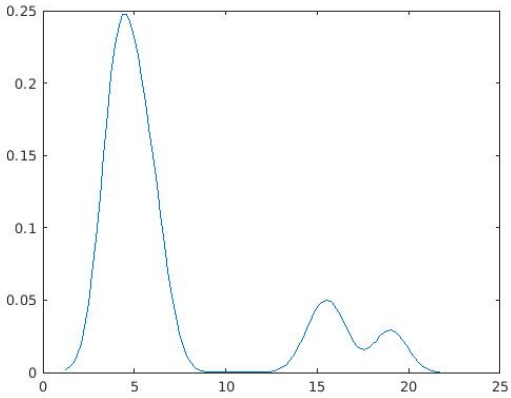


(a) KS density of lambdas, patient 1, RF1

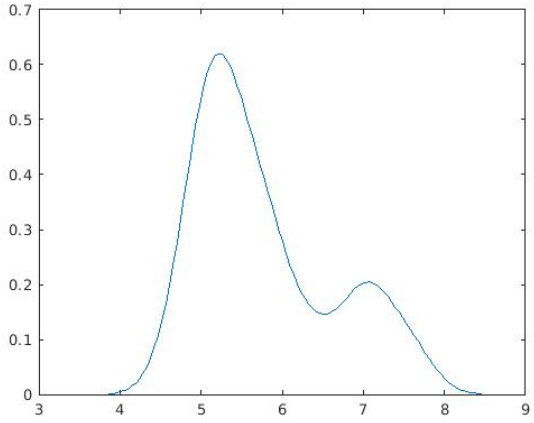


(b) KS density of Renyi entropies, patient 1, RF1

Figure 6: KS densities of lambdas and Renyi entropies for selected lines of patient 1

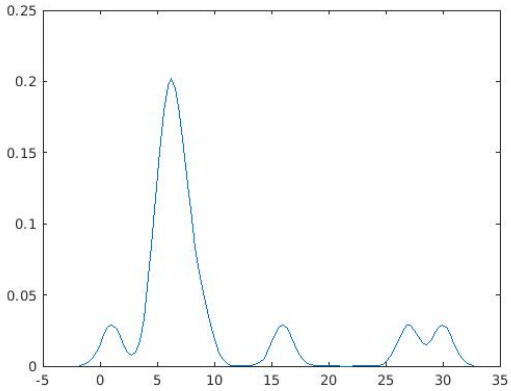


(a) KS density of lambdas, patient 4, RF1

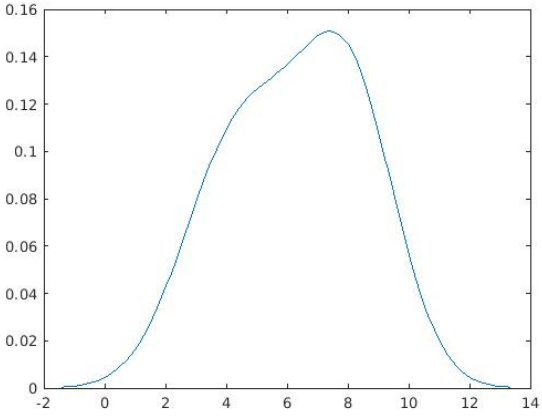


(b) KS density of Renyi entropies, patient 4, RF1

Figure 7: KS densities of lambdas and Renyi entropies for selected lines of patient 4

Although, initially, the decision to select fewer lines was made because of the computational heavyness of the full dataset, it turned out serving as a valuable exercise in how much a proper selection of the data can actually matter, and how many different observations we can get.

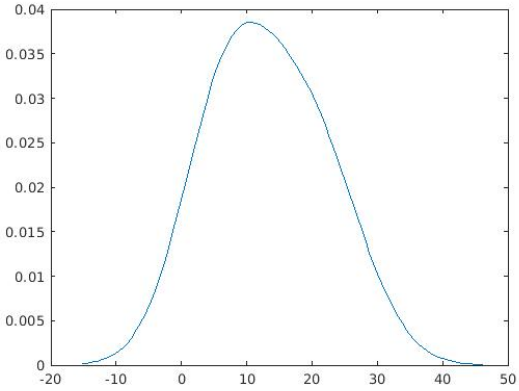


(a) KS density of lambdas, patient 23, RF1

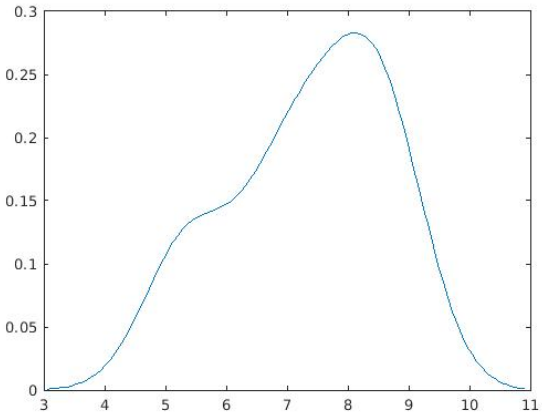


(b) KS density of Renyi entropies, patient 23, RF1

Figure 8: KS densities of lambdas and Renyi entropies for selected lines of patient 23

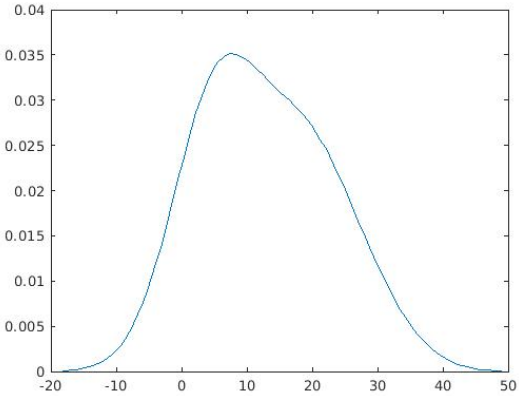


(a) KS density of lambdas, patient 69, RF1

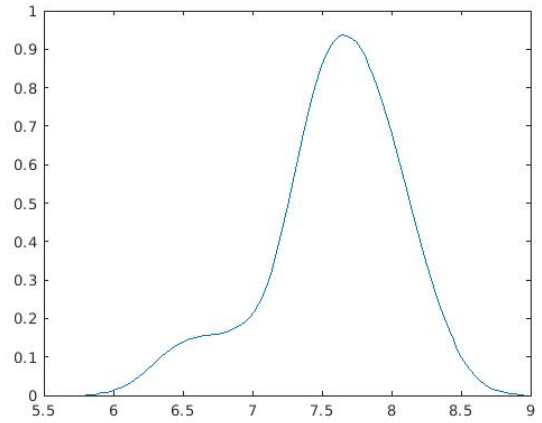


(b) KS density of Renyi entropies, patient 69, RF1

Figure 9: KS densities of lambdas and Renyi entropies for selected lines of patient 69

Focusing on the area around the strongest peak on the mesh grid, KS densities of optimal lambdas and their corresponding Renyi entropies change shape significantly, but, for optimal lambdas, the shapes are fairly similar, again indicating no strong difference between a malignant and benign lesion. The shape of the KS distributions for Renyi entropies, however, is very much different from the previous case, where now the RE for the malignant lesion has a more rounded shape with stronger variance, and significantly different means. All of that pertains to patients 1 (benign) and 4 (malignant).

Table 3: Mean, variance and standard deviation for optimal lambda for the selected lines of the dataset

| **PATIENT** | **mean** | **var** | **std** | **Classification** |
|---|---|---|---|---|
| Patient 1 RF1 | 7.1333 | 25.5524 | 5.0549 | Benign |
| Patient 1 RF2 | 10.6667 | 49.8095 | 7.0576 | Benign |
| Patient 4 RF1 | 9.7333 | 67.9238 | 8.2416 | Malignant |
| Patient 4 RF2 | 11.6667 | 55.5238 | 7.4514 | Malignant |
| Patient 23 RF1 | 13.2000 | 55.4571 | 7.4470 | Benign |
| Patient 23 RF2 | 13.6000 | 22.9714 | 4.7929 | Benign |
| Patient 69 RF1 | 12.800 | 77.7429 | 8.8172 | Malignant |
| Patient 69 RF2 | 12.8000 | 12.6952 | 3.5630 | Malignant |

Looking at KS densities for patients 23 and 69, we observe a much cleaner look for densities of optimal lambdas, both more centered and with larger variance than the previous benign/-malignant pair. KS densities of their respective Renyi entropies have now switched, with RE for patient 23 having a significantly larger variance than RE for patient 69. This kind of inconsistency in between patients suggests, again, that those are not good enough metrics to conclude which patient is diagnosed with a malignant tumor, and which one with a benign one.

Observing the data in Table 3, and Table 4 we can see those inconsistencies displayed across both RF1 and RF2 for both sets of patients.

Table 4: Mean, variance and standard deviation for optimal Renyi entropy for the selected lines of the dataset

| **PATIENT** | **mean** | **var** | **std** | **Classification** |
|---|---|---|---|---|
| Patient 1 RF1 | 5.7678 | 0.7180 | 0.8473 | Benign |
| Patient 1 RF2 | 6.5176 | 2.2181 | 1.4893 | Benign |
| Patient 4 RF1 | 6.2653 | 3.8621 | 1.9652 | Malignant |
| Patient 4 RF2 | 7.6799 | 0.4422 | 0.6650 | Malignant |
| Patient 23 RF1 | 7.3461 | 1.6187 | 1.2723 | Benign |
| Patient 23 RF2 | 7.1411 | 1.7567 | 1.3254 | Benign |
| Patient 69 RF1 | 7.5894 | 0.2027 | 0.4503 | Malignant |
| Patient 69 RF2 | 7.5894 | 1.3240 | 1.1507 | Malignant |

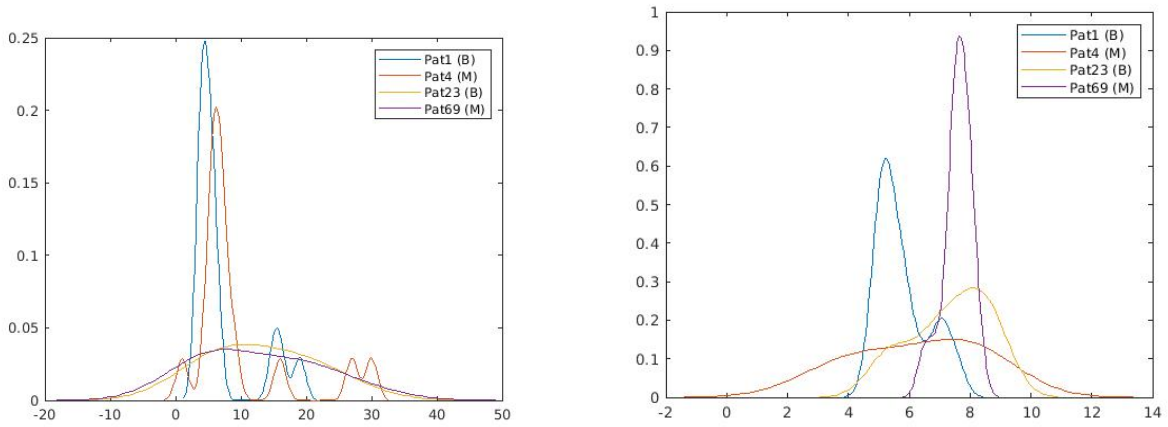


(a) KS density of optimal lambdas, RF1

(b) KS density of Renyi entropies, RF1

Figure 10: KS densities of lambdas and Renyi entropies for selected lines of all selected patients

## 3.2 Correlation

Selecting fewer lines, as well as selecting the equal amount of lines for each patient and RF echo plane, allowed us to look at the correlation between optimal lambdas/Renyi entropies within and across both scan planes.

Table 5: Correlation coefficients between RF1's for lambda

| | **PATIENT 1** | **PATIENT 4** | **PATIENT 23** | **PATIENT 69** | **Classification** |
|---|---|---|---|---|---|
| **PATIENT 1** | 1 | -0.1500 | -0.3613 | 0.4317 | Benign |
| **PATIENT 4** | | 1 | -0.3983 | -0.4018 | Malignant |
| **PATIENT 23** | | | 1 | 0.3749 | Benign |
| **PATIENT 69** | | | | 1 | Malignant |

Table 6: Correlation coefficients between RF2's for lambda

| | **PATIENT 1** | **PATIENT 4** | **PATIENT 23** | **PATIENT 69** | **Classification** |
|---|---|---|---|---|---|
| **PATIENT 1** | 1 | 0.5899 | -0.1922 | 0.1884 | Benign |
| **PATIENT 4** | | 1 | -0.4580 | 0.1946 | Malignant |
| **PATIENT 23** | | | 1 | -0.1514 | Benign |
| **PATIENT 69** | | | | 1 | Malignant |

Table 7: Correlation coefficients between RF1's for Renyi entropy

| | **PATIENT 1** | **PATIENT 4** | **PATIENT 23** | **PATIENT 69** | **Classification** |
|---|---|---|---|---|---|
| **PATIENT 1** | 1 | 0.7601 | 0.6854 | -0.1368 | Benign |
| **PATIENT 4** | | 1 | 0.8113 | -0.3054 | Malignant |
| **PATIENT 23** | | | 1 | -0.1073 | Benign |
| **PATIENT 69** | | | | 1 | Malignant |

Table 8: Correlation coefficients between RF2's for Renyi entropy

| | **PATIENT 1** | **PATIENT 4** | **PATIENT 23** | **PATIENT 69** | **Classification** |
|---|---|---|---|---|---|
| **PATIENT 1** | 1 | -0.2660 | 0.3943 | 0.6977 | Benign |
| **PATIENT 4** | | 1 | -0.2187 | 0.1780 | Malignant |
| **PATIENT 23** | | | 1 | -0.0370 | Benign |
| **PATIENT 69** | | | | 1 | Malignant |

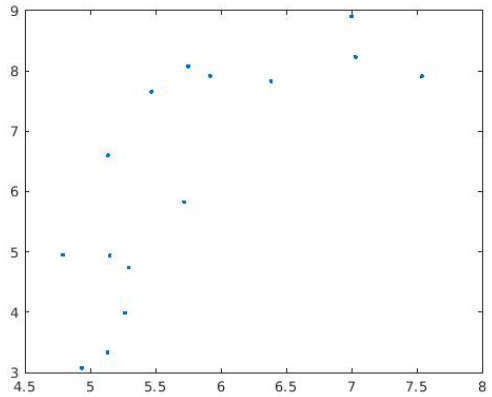


(a) Correlation of Renyi entropies between patients 1 and 4, RF1

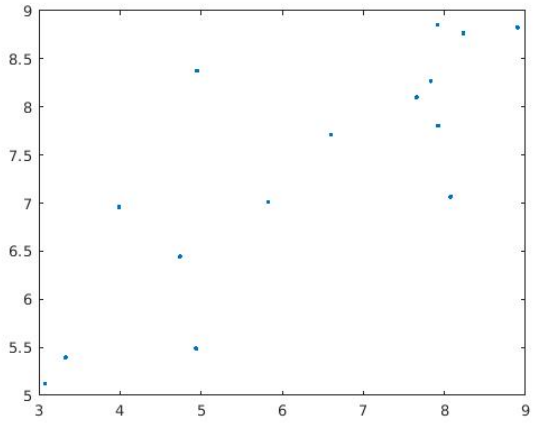


(b) Correlation of Renyi entropies between patients 4 and 23, RF1

Figure 11: Correlations of Renyi entropies between patients with malignant and benign lesions in RF1

Observing the correlation coefficients in Tables 5 to 8, we see the confirmation of trends noticed in the previous section, that is that there is very little correlation, positive or negative, between optimal lambdas/Renyi entropies of patients with malignant and benign tumors. There are, however, some noticeable exceptions, all pertaining to the Renyi entropy. Correlation between patients 1 and 4 in RF1 is 0.7601, between patients 4 and 23 in RF1 is 0.8113, and between patients 1 and 69 in RF 2 is 0.6977. All three have been plotted and presented in Figure 11 and Figure 12.

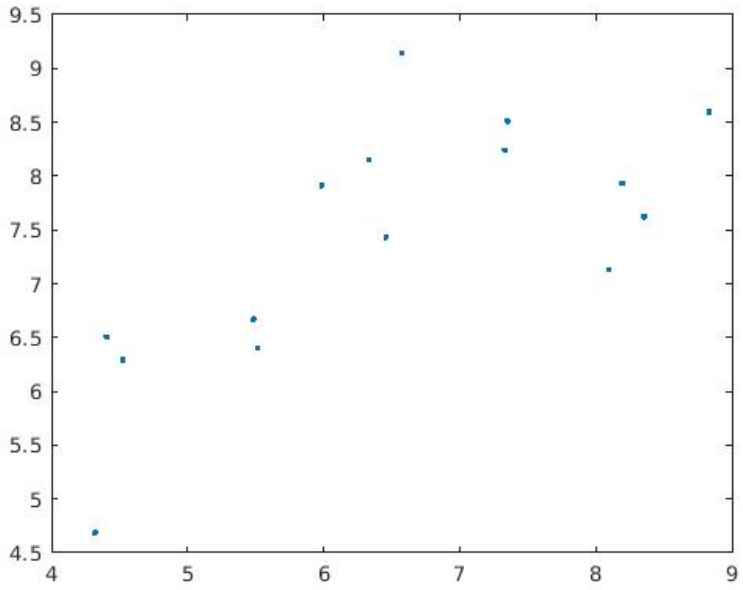


Figure 12: Correlation of Renyi entropies for patients 1 and 69 in RF2

# 4 Conclusions

Although some interesting observations can be made regarding the differences in Renyi entropy between the malignant and benign lesions, both on the full dataset, and on the shortened one, we would be slightly apprehensive about making definitive claims that it's a proper indicator of malignancy of a lesion. Mainly because of the outliers in the data and our inability to properly deal with them in this context, and their stronger impact on smaller number of RF echo lines. That also applies to optimal lambdas, who's variance between malignant and benign lesions is easily observable, and could potentially be an interesting metric to explore further. The random choice of patients could have also played a role in the obtained results. Study of larger number of patients, as well as dealing with outliers, should provide a better insight.

# 5 MATLAB code

```
load OASBUD.mat


%%
%rf1
%Extract patient data, all data lines

n=69; %patient number
m=190; %starting line

pat1_neg_rf1 = data(n).rf1;
pat1_rf1_clean = data(n).rf1 .* data(n).roi1;

roi_min=zeros(510,1);
roi_max=zeros(510,1);

for k=1:15

if mean(data(n).roi1(:,k+m))>0

roi_min(k)=min(find(data(n).roi1(:,k+m)));
roi_max(k)=max(find(data(n).roi1(:,k+m)));
Ysig(:,k)=pat1_rf1_clean(:,k+m);
end

end

%%
%rf2
n=69;
m=293; %starting line

pat1_neg_rf2 =data(n).rf2;
pat1_rf2_clean = data(n).rf2 .* data(n).roi2;

roi_min2=zeros(510,1);
roi_max2=zeros(510,1);

for k=1:15

if mean(data(n).roi2(:,k+m))>0

roi_min2(k)=min(find(data(n).roi2(:,k+m)));
roi_max2(k)=max(find(data(n).roi2(:,k+m)));
Ysig2(:,k)=pat1_rf2_clean(:,k+m);
end

end

%%


FFTL=1024; % FFT-length
Fs=40; % 40 MHz
%%
%rf1
f_min=3; % MHz
f_max=7; % MHz
```

```
fbin_min=round((f_min)/Fs*FFTL)
fbin_max=round((f_max)/Fs*FFTL)
%%
%rf2
f_min2=3;
f_max2=7;

fbin_min2=round((f_min2)/Fs*FFTL)
fbin_max2=round((f_max2)/Fs*FFTL)
%%
%rf1
lambdavect=[1:30]; % Parameter of the spectrogram window and scaled reassigned spectrogram
optimal_lambdavect=NaN(k,1); % Preallocated vector in which optimal lambdas will be stored
for k=1:15 % added another for loop to go through all of the lines

  if roi_max(k)-roi_min(k)~=0

    delta_t=2; % microsec

    tbin_min=roi_min(k);
    %tbin_max=roi_min(k)+round(delta_t*Fs);
    tbin_max=roi_max(k); % or roi_max


    for i=1:length(lambdavect)


      [MRS1,SS1,TI,FI]=crossMRS(Ysig(:,k),Ysig(:,k),lambdavect(i),FFTL,0,1);

      % Renyi for this lambda
      p=3;
      MRSc=MRS1([fbin_min:fbin_max],[tbin_min:tbin_max]);

      Stest=MRSc./sum(sum((MRSc)));
      Renyivect(i)=(1/(1-p)*log2(sum(sum(((Stest)).^p))));
      close all; %remove to produce all spectrogram images

    end

    [R,indmin]=min(Renyivect);

    'Optimal lambda'
    lambdavect(indmin)

    optimal_lambdavect(k)=lambdavect(indmin); %optimal lambdas appended one by one for each data
        line k
    k
  end
optimal_Renyivect(k)=min(Renyivect);
end

%%
%rf2
lambdavect2=[1:30]; % Parameter of the spectrogram window and scaled reassigned spectrogram
optimal_lambdavect2=NaN(k,1); % Preallocated vector in which optimal lambdas will be stored

for k=1:15

  if roi_max2(k)-roi_min2(k)~=0

    delta_t=2; % microsec
```

```
    tbin_min2=roi_min2(k);
    %tbin_max=roi_min(k)+round(delta_t*Fs);
    tbin_max2=roi_max2(k); % or roi_max


    for i=1:length(lambdavect2)


      [MRS1,SS1,TI,FI]=crossMRS(Ysig2(:,k),Ysig2(:,k),lambdavect2(i),FFTL,0,1);

      % Renyi for this lambda
      p=3;
      MRSc=MRS1([fbin_min2:fbin_max2],[tbin_min2:tbin_max2]);

      Stest=MRSc./sum(sum((MRSc)));
      Renyivect(i)=(1/(1-p)*log2(sum(sum(((Stest)).^p))));
      close all; %remove to produce all spectrogram images

    end

    [R,indmin]=min(Renyivect);

    'Optimal lambda'
    lambdavect2(indmin)

    optimal_lambdavect2(k)=lambdavect2(indmin); %optimal lambdas appended one by one for each data
        line k
    k
  end
optimal_Renyivect2(k)=min(Renyivect);
end

%%

lambda=lambdavect(indmin); % Parameter of the spectrogram window and scaled reassigned spectrogram

% MRS for the optimal lambda

[MRS1,SS1,TI,FI]=crossMRS(Ysig,Ysig,lambda,FFTL,0,1); %test with different lambdas

if max(max(SS1))>min(min(SS1))

figure
TI=TI/Fs;
FI=[0:FFTL/2-1]'/FFTL*Fs;
subplot(211)
cv=[min(min(SS1)) max(max(SS1))]
pcolor(TI,FI,SS1)
shading interp
caxis(cv)
ylabel('Frequency (MHz)')
xlabel('Time (microsec)')
title('Spectrogram')

subplot(212)
cv=[min(min(MRS1)) max(max(MRS1))/50]
pcolor(TI,FI,MRS1)
hold
plot(tbin_min*[1 1]/Fs,[0 0.5]*Fs,'r-')
plot(tbin_max*[1 1]/Fs,[0 0.5]*Fs,'r-')
plot([TI(1) TI(end)],f_min*[1 1],'r-')
plot([TI(1) TI(end)],f_max*[1 1],'r-')
```

```
hold
shading interp
caxis(cv)
ylabel('Frequency (MHz)')
xlabel('Time (microsec)')
title('MRS')

% Renyi for this lambda
p=3;
MRSc=MRS1([fbin_min:fbin_max],[tbin_min:tbin_max]);

Stest=MRSc./sum(sum((MRSc)));
Renyi=(1/(1-p)*log2(sum(sum(((Stest)).^p))))

else

    'Signal is zero'
end

%%

lambda2=lambdavect2(indmin); % Parameter of the spectrogram window and scaled reassigned
    spectrogram

% MRS for the optimal lambda

[MRS1,SS1,TI,FI]=crossMRS(Ysig2,Ysig2,lambda2,FFTL,0,1); %test with different lambdas

if max(max(SS1))>min(min(SS1))

figure
TI=TI/Fs;
FI=[0:FFTL/2-1]'/FFTL*Fs;
subplot(211)
cv=[min(min(SS1)) max(max(SS1))]
pcolor(TI,FI,SS1)
shading interp
caxis(cv)
ylabel('Frequency (MHz)')
xlabel('Time (microsec)')
title('Spectrogram')

subplot(212)
cv=[min(min(MRS1)) max(max(MRS1))/50]
pcolor(TI,FI,MRS1)
hold
plot(tbin_min*[1 1]/Fs,[0 0.5]*Fs,'r-')
plot(tbin_max*[1 1]/Fs,[0 0.5]*Fs,'r-')
plot([TI(1) TI(end)],f_min*[1 1],'r-')
plot([TI(1) TI(end)],f_max*[1 1],'r-')
hold
shading interp
caxis(cv)
ylabel('Frequency (MHz)')
xlabel('Time (microsec)')
title('MRS')

% Renyi for this lambda
p=3;
MRSc=MRS1([fbin_min2:fbin_max2],[tbin_min2:tbin_max2]);

Stest=MRSc./sum(sum((MRSc)));
```

```
Renyi=(1/(1-p)*log2(sum(sum(((Stest)).^p))))

else

    'Signal is zero'
end
```

# 6 Bibliography

[**1**] M. Sandsten: *Time-Frequency Analysis of Time-Varying Signals and Non-Stationary Processes*, Compendium, Lund University, 2022

[**2**] H. Piotrowska-Wroblewska, K. Dobruch-Sobczak, A. Nowicki - *Open access database of raw ultrasonic signals acquired from malignant and benign breast lesion*, American Association of Physicists in Medicine, Medical Physics, 44 (11), November 2017

[**3**] M. Sandsten, I. Reinhold, J. Starkhammar - *Objective detection and time-frequency localization of components within transient signals*, Journal of the Acoustical Society of America (JASA), vol. 143, no. 4, 2018.

[**4**] M. Sandsten, J. Brynolfsson - *The Scaled Reassigned Spectrogram with Perfect Localization for Estimation of Gaussian Functions*, IEEE Signal Processing Letters, vol. 22, no. 1, pp. 100–104, 2015.

[**5**] J. Starkhammar, I. Reinhold, T. Erlöv, M. Sandsten - *Scaled reassigned spectrogram applied to linear transducer signals*, JASA Express Lett. 1 (5), 052001 (2021)

[**6**] M. Sandsten, J. Brynolofsson, I. Reinhold - *The Matched Window Reassignment*, in EUSIPCO, Rome, Italy, 2018.

[**7**] World Cancer Research Fund International - *Worldwide cancer data*, https://www.wcrf.org/cancer-trends/worldwide-cancer-data/

[**8**] https://se.mathworks.com/help/stats/ksdensity.html